Exact stationary state of a run-and-tumble particle with three internal states in a harmonic trap

Urna Basu, Satya N. Majumdar, Alberto Rosso, Sanjib Sabhapandit, Gregory Schehr

Exact stationary state of a run-and-tumble particle with three internal states in a harmonic trap

Urna Basu[1], Satya N. Majumdar[2], Alberto Rosso[2], Sanjib Sabhapandit[1], Grégory Schehr[2]

[1]Raman Research Institute, Bengaluru 560080, India

[2]LPTMS, CNRS, Univ. Paris-Sud, Université Paris-Saclay, 91405 Orsay, France

Abstract. We study the motion of a one-dimensional run-and-tumble particle with three discrete internal states in the presence of a harmonic trap of stiffness μ. The three internal states, corresponding to positive, negative and zero velocities respectively, evolve following a jump process with rate γ. We compute the stationary position distribution exactly for arbitrary values of μ and γ which turns out to have a finite support on the real line. We show that the distribution undergoes a shape-transition as $\beta = \gamma/\mu$ is changed. For $\beta < 1$, the distribution has a double-concave shape and shows algebraic divergences with an exponent $(\beta - 1)$ both at the origin and at the boundaries. For $\beta > 1$, the position distribution becomes convex, vanishing at the boundaries and with a single, finite, peak at the origin. We also show that for the special case $\beta = 1$, the distribution shows a logarithmic divergence near the origin while saturating to a constant value at the boundaries.

1. Introduction

Recent years have seen a surge of interest in the study of active matter and active particles. The term 'active particle' refers to a class of self-propelled particles which can generate dissipative directed motion by consuming energy directly from their environment [1–6]. Examples of active matter can be found in nature at all length scales, ranging from micro-organisms like bacteria [7, 8] to granular matter [9, 10], flock of birds [11, 12] and fish-schools [13, 14]. Apart from a diverse set of novel collective behaviours like clustering [15–17], motility induced phase separation [18–20], and absence of well defined pressure [21], active particles show many intriguing features even at the single particle level. One such interesting feature is that, in the presence of external potentials and confining boundaries, active particles show very different behaviour than their passive counterparts, including non-Boltzmann stationary state, clustering near the boundaries of the confining region [22–26] and unusual relaxation and persistence properties [27–29]. There have been numerous recent studies focusing on the behaviour of active particles in the presence of external potentials and confinements, both theoretical [30–33] and experimental [34–37].

The theoretical attempts to characterise the behaviour of active particles focus on studying simple models of such systems. Run-and-tumble particle (RTP) is one of the most studied models of an active particle. An RTP is an overdamped particle which moves with a constant speed v_0, or 'runs,' along the direction of an internal 'spin' degree of freedom. The orientation of the spin can change randomly resulting in a sudden change, or 'tumble,' in the direction of motion of the particle. The simplest example is an RTP moving in one spatial dimension with two possible values of the spin $\sigma = \pm 1$. In this case, the particle moves with velocity v_0 or $-v_0$; the reversal of direction occurs stochastically with rate γ, with the flipping of the spin $\sigma \to -\sigma$. In the presence of an external potential $U(x)$, the position $x(t)$ of this two-state RTP evolves according to the Langevin equation,

$$\dot{x} = f(x) + v_0\sigma(t) \tag{1}$$

where $f(x) = -U'(x)$ is the deterministic force acting on the particle. The spin variable σ plays the role of the noise, its dichotomous nature giving rise to the 'activity'. In fact, it is clear from the auto-correlation $\langle \sigma(t)\sigma(t')\rangle = e^{-2\gamma|t-t'|}$ that $\sigma(t)$ is a coloured noise with a finite memory, characterised by the persistence time $\tau = (2\gamma)^{-1}$. Despite the apparent simplicity of the model, the two-state RTP shows a lot of intriguing features typical to active particles including non-Boltzmann stationary distribution [24, 27].

For any confining potential, the stationary position distribution of a two-state RTP is known exactly, and is given by,

$$P_{\rm st}(x) \propto \frac{1}{v_0^2 - f^2(x)} \exp\left[2\gamma \int_0^x {\rm d}y \frac{f(y)}{v_0^2 - f^2(y)}\right] \tag{2}$$

up to a normalization constant. The above result was first obtained long ago in the context of quantum optics [38–41], and later to study the role of coloured noise in dynamical systems [42]. More recently, it has been re-derived in the context of active particles [21, 24]. In particular, the stationary distribution (2) has been analysed for specific confining potentials of the type $U(x) \propto |x|^p$ with $p > 0$ in Ref. [24]. The case $p = 2$ corresponds to a harmonic potential which is of particular interest, not only from theoretical but also from an experimental point of view [35,37]. For a harmonic potential $U(x) = \mu x^2/2$, the stationary distribution (2) simplifies to,

$$P_{\rm st}(x) = \frac{2\mu}{4^\beta B(\beta,\beta) v_0} \left[1 - \left(\frac{\mu x}{v_0}\right)^2\right]^{\beta-1} \tag{3}$$

where $\beta = \gamma/\mu$ and $B(u, v)$ is the beta-function. This distribution is symmetric in x and has a finite support in the region $-\frac{v_0}{\mu} \le x \le \frac{v_0}{\mu}$. Consequently, the particle is confined within this region in the stationary state. This stationary position distribution shows an interesting shape-transition as a function of β. For $\beta > 1$ the distribution is convex shaped, with a peak at the origin $x = 0$ and $P_{\rm st}(x)$ vanishing at the boundaries $x = \pm\frac{v_0}{\mu}$. On the other hand, for $\beta < 1$ $P_{\rm st}(x)$ has a concave shape with divergences at the boundaries and a minimum at the origin. For $\beta = 1$, the distribution is uniform. Thus by varying β, one can observe a transition from a double-peaked (at the boundaries) to

a single-peaked distribution. The double-peaked nature of the distribution for $\gamma < \mu$ signifies an 'active phase', where the persistence time of the spin-orientation is larger than μ^{-1}, the relaxation time-scale of the potential. On the other hand, $\gamma > \mu$, *i.e.*, when the persistence time is smaller compared to μ^{-1}, corresponds to a passive phase, where the stationary distribution resembles that of a passive particle in a trap, with a single peak at the centre of the trap. Indeed, in the diffusive limit when $v_0 \to \infty$, $\gamma \to \infty$ but keeping the ratio $v_0^2/2\gamma = D$ fixed, the dynamics of the RTP in the harmonic trap converges to the Ornstein-Uhlenbeck process. This is also exhibited in the stationary state where the distribution in Eq. (3) converges to a Boltzmann distribution, which in this case is a simple Gaussian $P_{\rm st}(x) \propto e^{-\frac{\mu}{D}x^2}$.

It is then natural to ask how the stationary distribution changes if the RTP has more than two internal states. In fact, an RTP with many internal degrees have been studied where the internal degrees can take a set of discrete values and evolve following some discrete jump processes [43,44]. However, most of these studies are numerical and to the best of our knowledge no analytical results are available for the stationary state of a multi-state RTP in the presence of an external potential.

In this article, we study a run-and-tumble active particle in one spatial dimension with three discrete internal states, with positive, negative and zero velocities, respectively. We show that such a multi-state dynamics naturally arises when one considers an RTP in higher spatial dimensions and project it to one-dimension. We calculate exactly the stationary position probability distribution in the presence of a harmonic potential of strength μ for arbitrary flip-rate γ among the internal states. It turns out that the presence of the zero-velocity internal state leads to a rich behaviour of the position distribution $P(x)$. As in the two-state case, it turns out that the shape of the stationary state distribution is governed by one single parameter

$$\beta = \frac{\gamma}{\mu} \, . \tag{4}$$

We show that $P(x)$ has a finite support on the real line and undergoes a transition in shape as $\beta = \gamma/\mu$ is varied : For $\beta < 1$, $P(x)$ diverges both at the origin and the boundaries with the same exponent $\beta - 1$. Thus, in this case, the position distribution has a double-concave shape, with three peaks, namely at the boundaries and the origin. For $\beta = 1$, $P(x)$ shows a logarithmic divergence near the origin. On the other hand, for $\beta > 1$, the distribution converges to a finite value at the origin while it vanishes at the boundaries, implying a convex shape with a single peak at the origin (see Fig. 2).

2. Model

Our model of a three-state RTP in one-dimension is motivated by a natural "clock-like" model for a two-dimensional RTP. Let us indeed consider an overdamped particle moving on a two dimensional (xy) plane with an internal orientational degree of freedom or 'spin' σ associated with it. In the absence of any external potential the particle moves with a constant speed v_0 along the direction of σ, which is a unit vector with four possible

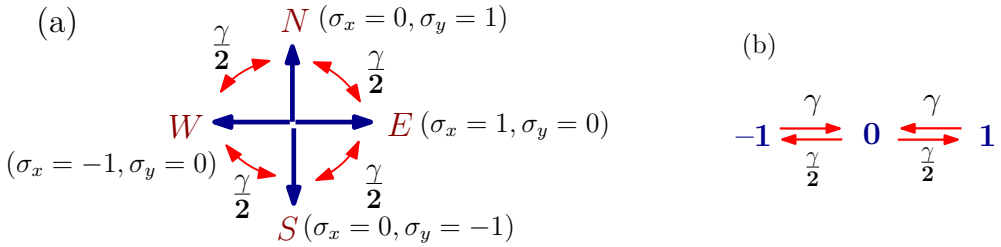

Figure 1. (a) Schematic representation of the jump process through which the orientation σ evolves. (b) The equivalent 3-state jump process for σ_x.

discrete orientations, denoted by E, W, N, S (along $\pm x$ and $\pm y$ axes respectively). The spin σ evolves in time following a Markov jump process – its orientation can change via a rotation of $\frac{\pi}{2}$ either clockwise or anti-clockwise, both with rate $\frac{\gamma}{2}$. This jump process is schematically represented in Fig. 1(a). Additionally, we consider an external harmonic potential $U(x,y) = \frac{\mu}{2}(x^2+y^2)$ which exerts a force $f(x,y) = -\nabla U(x,y)$ on the RTP.

The time-evolution of the position $(x(t), y(t))$ of the RTP can be conveniently expressed in terms of the Langevin equations,

$$\dot{x}(t) = -\mu x(t) + v_0 \sigma_x(t) \tag{5a}$$

$$\dot{y}(t) = -\mu y(t) + v_0 \sigma_y(t) \tag{5b}$$

where $\sigma_{x,y}(t)$ are components of the spin vector $\sigma(t)$ at any time t, along the x and y axes respectively (see Fig. 1(a)).

The position probability distribution $\mathcal{P}(x,y,t)$ is given by the sum $\mathcal{P}(x,y,t) = \sum_\sigma \mathcal{P}_\sigma(x,y,t)$ where $\mathcal{P}_\sigma(x,y,t)$ denotes the probability that the particle has the position (x,y) and orientation $\sigma = E, N, W, S$ at time t. These probabilities evolve according to the Fokker-Planck (FP) equations,

$$\frac{\partial}{\partial t}\mathcal{P}_E(x,y,t) = \frac{\partial}{\partial x}\Big[(\mu x - v_0)\mathcal{P}_E\Big] + \frac{\partial}{\partial y}\Big[\mu y \mathcal{P}_E\Big] + \frac{\gamma}{2}(\mathcal{P}_N + \mathcal{P}_S) - \gamma \mathcal{P}_E \tag{6a}$$

$$\frac{\partial}{\partial t}\mathcal{P}_N(x,y,t) = \frac{\partial}{\partial x}\Big[\mu x \mathcal{P}_N\Big] + \frac{\partial}{\partial y}\Big[(\mu y - v_0)\mathcal{P}_N\Big] + \frac{\gamma}{2}(\mathcal{P}_E + \mathcal{P}_W) - \gamma \mathcal{P}_N \tag{6b}$$

$$\frac{\partial}{\partial t}\mathcal{P}_W(x,y,t) = \frac{\partial}{\partial x}\Big[(\mu x + v_0)\mathcal{P}_W\Big] + \frac{\partial}{\partial y}\Big[\mu y \mathcal{P}_W\Big] + \frac{\gamma}{2}(\mathcal{P}_N + \mathcal{P}_S) - \gamma \mathcal{P}_W \tag{6c}$$

$$\frac{\partial}{\partial t}\mathcal{P}_S(x,y,t) = \frac{\partial}{\partial x}\Big[\mu x \mathcal{P}_S\Big] + \frac{\partial}{\partial y}\Big[(\mu y + v_0)\mathcal{P}_S\Big] + \frac{\gamma}{2}(\mathcal{P}_E + \mathcal{P}_W) - \gamma \mathcal{P}_S \tag{6d}$$

where we have suppressed the argument of P_σ on the right hand side for the sake of brevity. It is hard to find an analytical form of $\mathcal{P}(x,y,t)$ as these equations are difficult to solve, even in the stationary state.

However, it is also interesting to look at the x-process only, governed by Eq. (5a). This describes an effective one-dimensional RTP where the internal spin σ_x has three possible discrete values, $1, 0, -1$. As illustrated in Fig. 1(a), both $\sigma = N$ and $\sigma = S$ correspond to $\sigma_x = 0$ while $\sigma = E$ and $\sigma = W$ corresponds to $\sigma_x = 1$ and $\sigma_x = -1$, respectively. The jump from $\sigma_x = 1$ to 0 can, thus, occur through two different channels ($E \to N$ and $E \to S$), resulting in a jump rate γ for $\sigma_x = 1 \to \sigma_x = 0$. Similarly,

$\sigma_x = -1 \to \sigma_x = 0$ occurs with rate γ, while $0 \to \pm 1$ occurs with rate $\frac{\gamma}{2}$ (since there is only one way to make this transition). This effective 3-state jump process in one-dimension is schematically shown in Fig. 1(b). Let $P_i(x,t)$ denote the probability that the RTP is at a position x at time t with $\sigma_x = i$. The corresponding FP equations read,

$$\frac{\partial}{\partial t}P_1(x,t) = \frac{\partial}{\partial x}[(\mu x - v_0)P_1] + \frac{\gamma}{2}P_0 - \gamma P_1 \tag{7a}$$

$$\frac{\partial}{\partial t}P_{-1}(x,t) = \frac{\partial}{\partial x}[(\mu x + v_0)P_{-1}] + \frac{\gamma}{2}P_0 - \gamma P_{-1} \tag{7b}$$

$$\frac{\partial}{\partial t}P_0(x,t) = \frac{\partial}{\partial x}[\mu x P_0] + \gamma(P_1 + P_{-1}) - \gamma P_0. \tag{7c}$$

We note that this set of FP equations can also be obtained from Eqs. (6a)-(6d) by integrating both sides over y and then identifying $P_1(x,t) = \int \mathrm{d}y\ \mathcal{P}_E(x,y,t)$, $P_{-1}(x,t) = \int \mathrm{d}y\ \mathcal{P}_W(x,y,t)$, and $P_0(x,t) = \int \mathrm{d}y\ [\mathcal{P}_N(x,y,t) + \mathcal{P}_S(x,y,t)]$.

In the presence of the confining harmonic potential, in the long time limit the RTP is expected to reach a stationary state where the left hand side (l. h. s.) of the Eqs. (7a) - (7c) would vanish. The corresponding stationary distributions $P_i(x) = \lim_{t\to\infty} P_i(x,t)$ then satisfy a set of coupled linear differential equations (obtained by putting $\frac{\partial P_i}{\partial t} = 0$),

$$\frac{\mathrm{d}}{\mathrm{d}x}[(\mu x - v_0)P_1] + \frac{\gamma}{2}P_0 - \gamma P_1 = 0 \tag{8a}$$

$$\frac{\mathrm{d}}{\mathrm{d}x}[(\mu x + v_0)P_{-1}] + \frac{\gamma}{2}P_0 - \gamma P_{-1} = 0 \tag{8b}$$

$$\frac{\mathrm{d}}{\mathrm{d}x}[\mu x P_0] + \gamma(P_1 + P_{-1}) - \gamma P_0 = 0. \tag{8c}$$

Our objective is to solve this set of equations to find $P_i(x)$ in the stationary state.

Boundary Conditions: To proceed with the solution we first need to specify the boundary conditions for $P_i(x)$. To determine these boundary conditions, we first note that, in the stationary state, the RTP is confined within a finite region bounded by $x_\pm = \pm v_0/\mu$. This can be understood easily from the following argument: from the Langevin equation (5a) it is clear that if the particle is outside the region $[x_-, x_+]$, it always feels a drift towards the origin, irrespective of the value of σ_x. As a result, if the particle starts from some initial position $x_0 > x_+$, or $x_0 < x_-$, it will eventually reach the region $[x_-, x_+]$. Consequently, the stationary distribution has a finite support in the region $[x_-, x_+]$ and it is zero outside. To solve Eqs. (8a) - (8c) then, we need to specify the boundary conditions at these two points. Let us first look at the behaviour of $P_1(x)$ near $x = x_-$. During an infinitesimal time increment Δt, $P_1(x_-, t)$ evolves as,

$$P_1(x_-, t + \Delta t) = (1 - \gamma\Delta t)P_1(x_- - \Delta x, t) + \frac{\gamma}{2}\Delta t P_0(x_-, t) \tag{9}$$

where the first term on the right hand side (r.h.s.) represents the transition when the position of the particle changes by an amount Δx during interval Δt, and the second term corresponds to the case when σ_x changes from 0 to 1; the pre-factors $(1 - \gamma\Delta t)$ and $\gamma\Delta t/2$ denotes the probabilities for these two occurrences, respectively. Now, in the

stationary state, the probabilities $P_i(x)$ are independent of time, hence, we have from (9),

$$P_1(x_-) = (1-\gamma\Delta t)P_1(x_- - \Delta x) + \frac{\gamma}{2}\Delta t P_0(x_-) \tag{10}$$

Moreover, from Eq. (5a) we have, for $\sigma_x = 1$ and near x_-, $\Delta x \simeq (-\mu x_- + v_0)\Delta t = 2v_0\Delta t > 0$, thus $P_1(x_- - \Delta x) = P_1(x_- - 2v_0\Delta t)$ which vanishes in the stationary state, as the argument $x_- - 2v_0\Delta t$ is outside the region $[x_-, x_+]$. Then, taking $\Delta t \to 0$ limit in Eq. (10), we get $P_1(x_-) = 0$. Using similar arguments for P_{-1} and P_0, one finds the full set of boundary conditions to be satisfied by the set of equations (8a) - (8c),

$$P_1(x_-) = 0,\ P_{-1}(x_+) = 0,\ P_0(x_-) = 0,\ P_0(x_+) = 0. \tag{11}$$

Note that the behaviour of $P_1(x_+)$ and $P_{-1}(x_-)$ remain unspecified. The set of boundary conditions for P_1 and P_{-1} is very similar to the case of 2-state RTP [24]. However, as we will see below, the presence of the third state $\sigma_x = 0$ leads to a richer behaviour in the present case.

3. Exact Solution

The straightforward strategy to solve a set of coupled first order equations like Eqs. (8a) - (8c) is to decouple them and find separate equations for $P_i(x)$. However, our primary goal is to find the marginal position distribution of the particle, *i.e.*, the probability that the effective one-dimensional RTP has a position x, irrespective of the spin-orientation σ_x. This is given by

$$P(x) = P_0(x) + P_1(x) + P_{-1}(x). \tag{12}$$

In the following we attempt to derive an equation for $P(x)$ using Eqs. (8a) - (8c). To this end, we first define,

$$Q(x) = P_1(x) + P_{-1}(x), \quad \text{and} \quad R(x) = P_1(x) - P_{-1}(x). \tag{13}$$

It is straightforward to see that in terms of these functions P and Q, the four boundary conditions given by Eq. (11) translate to,

$$P(x_+) = Q(x_+), \quad \text{and } P(x_-) = Q(x_-) \tag{14}$$

Note that the boundary conditions of $R(x)$ remain unspecified. We proceed by expressing Eqs. (8a) - (8c) in terms of these functions P and Q. For this purpose, we first add equations (8a), (8b) and (8c) to get,

$$\frac{\mathrm{d}}{\mathrm{d}x}\Big[\mu x P(x) - v_0 R(x)\Big] = 0 \ \Rightarrow \mu x P(x) - v_0 R(x) = C \tag{15}$$

where C is a constant independent of x. To determine C, we substitute $x = x_+$ in the above equation. Using the definitions of P and R, along with the boundary condition (11), we get, $C = (\mu x_+ - v_0)P_1(x_+) = 0$. Hence, from Eq. (15) we have,

$$R(x) = \frac{\mu x}{v_0} P(x) \tag{16}$$

for all values of x. Now, adding Eqs. (8a) and (8b) and using Eq. (16), we get,

$$\mu x P'(x) + (\mu - \gamma)P(x) = \mu x Q'(x) + (\mu - 2\gamma)Q(x) \tag{17}$$

where $'$ denotes the derivative with respect to (w.r.t.) the argument of the functions. Next, we subtract Eq. (8b) from Eq. (8a) to get,

$$(\mu x)^2 P'(x) + \mu(2\mu - \gamma)xP(x) = v_0^2 Q'(x). \tag{18}$$

Eqs. (17) and (18) are two coupled linear differential equations involving $P(x)$ and $Q(x)$. In the following, we use them to get two separate differential equations for $P(x)$ and $Q(x)$. But, first, it is convenient to use a change of variable $z = (\frac{\mu x}{v_0})^2$ with $0 \le z \le 1$. Let us denote $\tilde{P}(z) = P(x = v_0\sqrt{z}/\mu)$ and $\tilde{Q}(z) = Q(x = v_0\sqrt{z}/\mu)$. Eqs. (17) and (18) then become,

$$2z\tilde{P}'(z) + (1-\beta)\tilde{P}(z) \quad = 2z\tilde{Q}'(z) + (1-2\beta)\tilde{Q}(z) \tag{19}$$

$$z\tilde{P}'(z) + \left(1 - \frac{\beta}{2}\right)\tilde{P}(z) = \tilde{Q}'(z) \tag{20}$$

where $\beta = \gamma/\mu$. The two boundary conditions in Eq. (14) reduce to a single condition for $\tilde{P}$ and $\tilde{Q}$,

$$\tilde{P}(z=1) = \tilde{Q}(z=1)\ . \tag{21}$$

As we will see below, this boundary condition is enough to solve the differential equations uniquely.

To get an equation involving $\tilde{P}(z)$ only, we take derivative of Eq. (19) w.r.t. z. Then, using Eq. (20), we immediately arrive at a second order differential equation,

$$z(1-z)\tilde{P}''(z) + \left[\frac{3-\beta}{2} - \frac{1}{2}(7-3\beta)z\right]\tilde{P}'(z) - \left(1-\frac{\beta}{2}\right)\left(\frac{3}{2}-\beta\right)\tilde{P}(z) = 0 \tag{22}$$

It is straightforward to check that the above equation is in the form of a hypergeometric differential equation,

$$z(1-z)\tilde{P}''(z) + [c_1 - (a_1 + b_1 + 1)z]\tilde{P}'(z) - a_1 b_1 \tilde{P}(z) = 0 \tag{23}$$

with the parameters,

$$a_1 = 1 - \frac{\beta}{2}; \quad b_1 = \frac{3}{2} - \beta; \quad c_1 = \frac{3-\beta}{2}. \tag{24}$$

One can also get a similar second order equation for $\tilde{Q}(z)$. To this end, we first express $P'(z)$ in terms of $\tilde{Q}(z)$ and $\tilde{Q}'(z)$, *i.e.*, in a form similar to Eq. (20). Multiplying Eq. (19) by $(1 - \frac{\beta}{2})$ and Eq. (20) by $(1-\beta)$, and subtracting the latter resulting equation from the former, we get,

$$z\tilde{P}'(z) = (1-2\beta)\left(1-\frac{\beta}{2}\right)\tilde{Q} - [1 - \beta - (2-\beta)z]\tilde{Q}'(z) \tag{25}$$

Taking a derivative of Eq. (20) and using Eq. (25), we get,

$$z(1-z)\tilde{Q}''(z) + \left[\frac{1-\beta}{2} - \frac{1}{2}(5-3\beta)z\right]\tilde{Q}'(z) - \left(1-\frac{\beta}{2}\right)\left(\frac{1}{2}-\beta\right)\tilde{Q}(z) = 0 \tag{26}$$

Clearly, this is also a hypergeometric differential equation of the form (23), but with a different parameter set,

$$a_2 = 1 - \frac{\beta}{2} = a_1, \quad b_2 = \frac{1}{2} - \beta = b_1 - 1, \quad c_2 = \frac{1-\beta}{2} = c_1 - 1. \tag{27}$$

3.1. Position distribution for $\beta \neq 1$

The general solutions for Eqs. (22) and (26) can be written in terms of the hypergeometric function ${}_2F_1(a, b, c; z)$ [45]. For $c_1 \neq 1$, *i.e.*, for $\beta \neq 1$, these general solutions read,

$$P(z) = A_1 \ [{}_2F_1(a_1, b_1, c_1; z)] + B_1 z^{1-c_1} \ [{}_2F_1(a_1 - c_1 + 1, b_1 - c_1 + 1, 2 - c_1; z)] \tag{28}$$

$$Q(z) = A_2 \ [{}_2F_1(a_2, b_2, c_2; z)] + B_2 z^{1-c_2} \ [{}_2F_1(a_2 - c_2 + 1, b_2 - c_2 + 1, 2 - c_2; z)] \tag{29}$$

where A_1, A_2, B_1, B_2 are arbitrary constants. The case $\beta = 1$ is special, which we discuss later. To determine the constants A_1, A_2, B_1, B_2, we first use the original first order equations (19) and (20) which must be satisfied by the solution. Substituting Eqs. (28) and (29) in Eq. (20) and using well known identities involving the hypergeometric function, we get, $B_2 = \frac{B_1}{1+\beta}$ and $A_2 = \frac{A_1(1-\beta)}{1-2\beta}$. Next, we impose the boundary condition (21). Once again, using properties of hypergeometric functions, we get

$$B_1 = \frac{2A_1}{\sqrt{\pi}} \frac{\Gamma(\frac{3-\beta}{2})\Gamma(\frac{1}{2}+\beta)}{(1-2\beta)\Gamma(\frac{1+\beta}{2})} \tag{30}$$

To completely specify $\tilde{P}(z)$ we still need A_1 which can be determined using the normalization condition,

$$\int_{x_-}^{x_+} \mathrm{d}x \ P(x) = 1 \Rightarrow \int_0^{v_0/\mu} \mathrm{d}x \ \tilde{P}\left[\left(\frac{\mu x}{v_0}\right)^2\right] = \frac{1}{2}. \tag{31}$$

Fortunately, this integral can be performed analytically and yields,

$$A_1 = \frac{\mu}{2v_0}\left[{}_3F_2\left(\begin{matrix}\frac{1}{2} & \frac{3}{2}-\beta & 1-\frac{\beta}{2} \\ \frac{3}{2} & \frac{3-\beta}{2} & \end{matrix}; 1\right) - \frac{1}{\beta\sqrt{\pi}} \frac{\Gamma(\frac{3-\beta}{2})\Gamma(\beta-\frac{1}{2})}{\Gamma(\frac{1+\beta}{2})} \ {}_3F_2\left(\begin{matrix}\frac{1}{2} & 1-\frac{\beta}{2} & \frac{\beta}{2} \\ \frac{1+\beta}{2} & \frac{\beta}{2}+1 & \end{matrix}; 1\right)\right]^{-1} \tag{32}$$

where ${}_pF_q\left(\begin{smallmatrix}a_1, a_2, \ldots a_p \\ b_1, b_2, \ldots b_q\end{smallmatrix}; z\right)$ denotes the generalized hypergeometric function [45]. Finally, we can write an explicit expression for the stationary position probability distribution,

$$P(x) = A_1 \left[{}_2F_1\left(1-\frac{\beta}{2}, \frac{3}{2}-\beta, \frac{3-\beta}{2}; \left(\frac{\mu x}{v_0}\right)^2\right) + \frac{2}{\sqrt{\pi}} \frac{\Gamma(\frac{3-\beta}{2})\Gamma(\beta+\frac{1}{2})}{(1-2\beta)\Gamma(\frac{\beta+1}{2})} \left(\frac{\mu x}{v_0}\right)^{\beta-1} {}_2F_1\left(\frac{1}{2}, 1-\frac{\beta}{2}, \frac{\beta+1}{2}; \left(\frac{\mu x}{v_0}\right)^2\right)\right] \tag{33}$$

where the normalization constant A_1 is given by Eq. (32). Note that, $P(x)$ is an even function of x and it depends on the flip rate γ comes through the ratio $\beta = \gamma/\mu$ only.

$P(x)$ takes particularly simple form for certain specific values of β,

$$P(x) = \begin{cases} \frac{\Gamma(\frac{3}{4})}{\sqrt{\pi}\Gamma(\frac{1}{4})} \frac{\sqrt{\mu v_0}}{\sqrt{|x|(v_0^2-\mu^2x^2)}} & \text{for} \quad \beta = \frac{1}{2} \\ \frac{\mu}{v_0}(1-\frac{\mu|x|}{v_0}) & \text{for} \quad \beta = 2 \\ \frac{6\mu}{5v_0}\left[1-5(\frac{\mu x}{v_0})^2 - \left(\frac{\mu|x|}{v_0}\right)^3\left((\frac{\mu x}{v_0})^2-5\right)\right] & \text{for} \quad \beta = 4. \end{cases} \tag{34}$$

One can also write an explicit expression for $Q(x)$ using Eqs.(29) and (30),

$$Q(x) = \frac{A_1}{(1-2\beta)}\left[(1-\beta)\ {}_2F_1\left(1-\frac{\beta}{2}, \frac{1}{2}-\beta, \frac{1-\beta}{2}; \left(\frac{\mu x}{v_0}\right)^2\right)\right.$$
$$\left. + \frac{2}{\sqrt{\pi}} \frac{\Gamma(\frac{3-\beta}{2})\Gamma(\beta+\frac{1}{2})}{(1+\beta)\Gamma(\frac{\beta+1}{2})} \left(\frac{\mu x}{v_0}\right)^{\beta+1}\ {}_2F_1\left(\frac{1}{2}, 1-\frac{\beta}{2}, \frac{\beta+3}{2}; \left(\frac{\mu x}{v_0}\right)^2\right)\right]. \tag{35}$$

From Eqs. (33) and (35) and using the relation (16) between $P(x)$ and $R(x)$ we can also calculate $P_i(x)$ individually in a straightforward manner. However, we do not give explicit expressions for them here. Figure 2(a) and (c) show plots of $P(x)$ as a function of x for different values of β calculated from Eq. (33) along with the data obtained from numerical simulations. It appears that, similar to the 2-state RTP, the distribution shows two different behaviours near the boundary $x = x_\pm$ depending on the value of β. Moreover, it appears from the plots that for $\beta < 1$, $P(x)$ also diverges near the origin $x = 0$ while it shows a cusp-like behaviour for large β. In the following we investigate the behaviour of $P(x)$ in more details and characterise this change in shape.

Behaviour near $x = 0$: To understand the behaviour of $P(x)$ near the origin we use the series expansion of the hypergeometric function ${}_2F_1(a, b, c; z)$ near $z = 0$,

$${}_2F_1(a, b, c; z) = 1 + \frac{ab}{c}z + \frac{ab(1+a)(1+b)}{2c(1+c)}z^2 + \mathcal{O}(z^3) \tag{36}$$

Using this expansion in Eq. (33), we have, near $x = 0$,

$$P(x) \sim \begin{cases} B_1\left(\frac{\mu}{v_0}x\right)^{\beta-1} & \text{for } \beta < 1 \\ A_1(1-C_1x^{\beta-1}) & \text{for } 1 < \beta < 3 \\ A_1(1-C_2x^2) & \text{for } \beta > 3 \end{cases} \tag{37}$$

where B_1 and A_1 are given respectively in Eqs. (30) and (32) while C_1 and C_2 are given by

$$C_1 = \frac{2}{\sqrt{\pi}} \frac{\Gamma(\frac{3-\beta}{2})\Gamma(\beta+\frac{1}{2})}{(2\beta-1)\Gamma(\frac{\beta+1}{2})} \left(\frac{\mu}{v_0}\right)^{\beta-1}, \tag{38}$$

$$C_2 = \frac{2\beta^2+6-7\beta}{2(\beta-3)} \left(\frac{\mu}{v_0}\right)^2. \tag{39}$$

Clearly, for $\beta < 1$, $P(x)$ diverges near the origin whereas for $\beta > 1$ it approaches a finite value. The approach also depends on the value of β : for $1 < \beta < 3$, $P(x)$ has a cusp-like behaviour near the origin while for $\beta \geq 3$ it shows a quadratic behaviour,

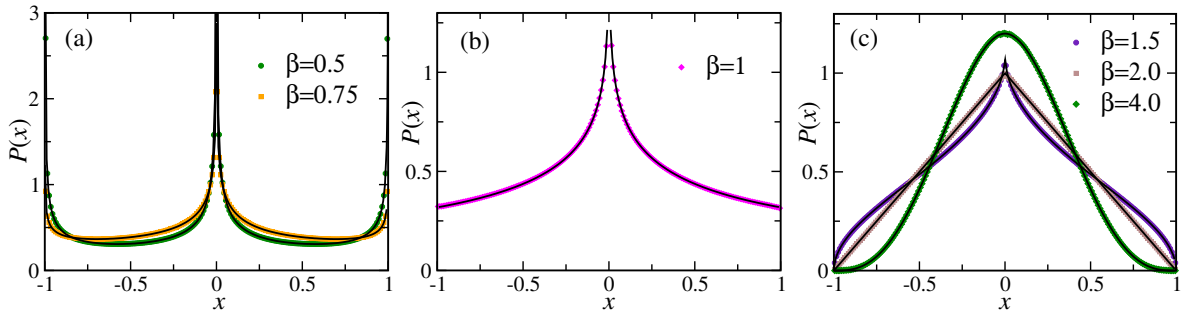

Figure 2. Stationary position distribution $P(x)$ as a function of x for the 3-state model for (a) $\beta < 1$, (b) $\beta = 1$, and (c) $\beta > 1$. Here $v_0 = 1$ and $\mu = 1$. The symbols correspond to the data obtained from numerical simulations while solid lines are obtained from the exact result [see Eq. (33) and Eq. (46)].

resembling a Gaussian around the origin. Indeed, in the diffusive limit, when $\gamma \to \infty$ and $v_0 \to \infty$ keeping $v_0^2/(2\gamma) = D$ fixed (as a consequence $\beta \to \infty$ in this limit), we find from Eq. (39) that $C_2 \to \mu/(2D)$. As a result, from the third line of (37), we recover the Boltzmann distribution $P(x) \sim e^{-\mu/(2D)x^2}$ which actually holds for all x.

Behaviour near $x = x_\pm$: The position distribution $P(x)$ also shows an interesting behaviour near the boundaries $x = x_\pm$. As $P(x)$ is symmetric in x, it suffices to explore its nature near one boundary, say x_+. To characterise the same we use the series expansion of ${}_2F_1(a, b, c; z)$ near $z = 1$. From Eq. (28), we have, for $z \to 1^-$,

$$\tilde{P}(z) \sim \begin{cases} (1-z)^{\beta-1} & \text{for } \beta < 3 \\ (1-z)^2 & \text{for } \beta > 3 \\ \cdot & \end{cases} \tag{40}$$

Hence, near $x = x_+$, we have the following behaviour of $P(x)$:

$$P(x) \sim \begin{cases} (x_+ - x)^{\beta-1} & \text{diverges for } \beta < 1 \\ (x_+ - x)^{\beta-1} & \text{vanishes for } 1 < \beta \leq 3 \\ (x_+ - x)^2 & \text{vanishes for } \beta > 3\,. \end{cases} \tag{41}$$

A similar behaviour is seen also near $x = x_-$. Note that this "freezing" for the leading behaviour for $\beta > 3$ occurs only for the three-state model, but not for the two-state model [24].

3.2. Position distribution for $\beta = 1$

As mentioned before, the case $\beta = 1$ is special. In this case, the differential equations (22) and (26) reduce to,

$$z(1-z)\tilde{P}''(z) + (1-2z)\tilde{P}'(z) - \frac{1}{4}\tilde{P}(z) = 0 \tag{42}$$

$$z(1-z)\tilde{Q}''(z) - z\tilde{Q}'(z) + \frac{1}{4}\tilde{Q}(z) = 0. \tag{43}$$

which correspond to two hypergeometric equations with $c_1 = 1$ and $c_2 = 0$, along with $a_1 = a_2 = b_1 = 1/2, b_2 = -1/2$. Eq. (28) is not a general solution anymore as the two hypergeometric functions therein become identical. We use Mathematica to solve Eqs. (42) and (43) and it turns out that the general solutions can be expressed in the form,

$$\tilde{P}(z) = \frac{2A_1}{\pi} K(1-z) + B_1 \mathcal{Q}_{-\frac{1}{2}}(2z-1) \tag{44}$$

$$\tilde{Q}(z) = A_2 z \; {}_2F_1\left(\frac{1}{2}, \frac{3}{2}, 2; z\right) + B_2 \; G^{20}_{22}\left(\begin{matrix}\frac{1}{2} & \frac{3}{2} \\ 0 & 1\end{matrix}; z\right). \tag{45}$$

Here $K(u)$ is the Legendre's complete elliptic integral of the first kind (see Ref. [46] and Eq. 19.2.8 in Ref. [45]), $G^{mn}_{pq}\left(\begin{smallmatrix} a_1,\ldots a_p \\ b_1 \ldots b_q \end{smallmatrix}; z\right)$ is the Meijer's G-function (see Ref. [46] and Eq. 16.17.1 in Ref. [45]) and $\mathcal{Q}_\nu(u)$ is the Legendre function of the second kind (see Eq. 14.3.7 in Ref. [45]).

To determine the arbitrary constants A_1, A_2, B_1 and B_2 we use the same strategy as in the previous section. First, we note that the solutions in Eqs. (44) and (45) must satisfy the original first order equations (19) and (20) with $\beta = 1$ for all values of z. We then look at the behaviour of $\tilde{P}(z)$ and $\tilde{Q}(z)$ in Eqs. (44) and (45) near $z = 0$. In this limit both $K(1-z)$ and $G^{20}_{22}\left(\begin{smallmatrix}\frac{1}{2} & \frac{3}{2} \\ 0 & 1\end{smallmatrix}; z\right)$ diverge logarithmically whereas the Legendre and hypergeometric functions approach a constant value. Substituting the series expansions of these functions back into Eq. (20) and comparing coefficients of $\ln z$ and different powers of z, we get, $B_2 = A_1$, and $A_2 = -\frac{\pi}{4} B_1$. It is also straightforward to check that Eq. (19) gives the same relation. We still have two independent constants A_1 and B_1. To determine these we use the boundary condition (21). Using the limiting behaviours of the special functions we have, for $z \to 1^-$, $\tilde{P}(z) - \tilde{Q}(z) = B_1 + \mathcal{O}(1-z)$ which immediately implies $B_1 = 0$ [see Eq. (21)]. The last remaining constant A_1 can be determined from the normalization condition (31) and yields $A_1 = \frac{\mu}{\pi v_0}$. Finally, we have, for $\beta = 1$,

$$P(x) = \frac{2\mu}{\pi^2 v_0} K\left(1 - \frac{\mu^2 x^2}{v_0^2}\right), \quad \text{and} \quad Q(x) = \frac{\mu}{\pi v_0} G^{20}_{22}\left(\begin{matrix}\frac{1}{2} & \frac{3}{2} \\ 0 & 1\end{matrix}; \frac{\mu^2 x^2}{v_0^2}\right). \tag{46}$$

Figure 2(b) shows a plot of $P(x)$ for $\beta = 1$ together with the same obtained from numerical simulations. To understand the behaviour near the origin $x = 0$ and the boundaries $x = x_\pm$ we look at the series expansion of $P(x)$. Near $x = 0$, a logarithmic divergence is seen, $P(x) \sim -\ln x$. On the other hand, near the boundaries $x = x_\pm$, $P(x)$ approaches a constant value, $\lim_{x \to x_\pm} P(x) = \frac{\mu}{\pi v_0}$.

4. Conclusion

In this paper, we have solved exactly the stationary position distribution of a one-dimensional run-and-tumble (RTP) particle with three discrete internal states and subjected to an external harmonic potential. To our knowledge, this is the first exact solution with three states that generalizes the well-known result for the standard two-state RTP. We showed that the stationary state exhibits a rich behavior as a function of

the single parameter $\beta = \gamma/\mu$ (where γ represents the rate at which the internal state changes and μ is the stiffness of the trap). One of the interesting outcomes is that the stationary distribution undergoes a shape-transition at $\beta = 1$.

While we were able to characterise the stationary state of a three-state RTP in a harmonic trap exactly, it would be interesting to study the relaxational dynamics towards this stationary state, as was recently done for the two-state RTP [24]. It would also be natural to extend our studies to non-harmonic potentials, such as $U(x) \sim |x|^p$, with $p > 0$. Another natural extension would be to consider an RTP particle with more than 3 internal states. Finding even the stationary state of a general n-state RTP with $n > 3$ remains a challenging open problem.

Acknowledgments

We acknowledge support from the project 5604-2 of the Indo-French Centre for the Promotion of Advanced Research (IFCPAR). S. N. M. acknowledges the support from the Science and Engineering Research Board (SERB, government of India) under the VAJRA faculty scheme (Ref.VJR/2017/000110) during a visit to the Raman Research Institute in 2019, where part of this work was carried out. U. B. acknowledges support from Science and Engineering Research Board (SERB), India under Ramanujan Fellowship (Grant No. SB/S2/RJN-077/2018) and CNRS for a one month visit to LPTMS, Univ. Paris-Sud.

[1] P. Romanczuk, M. Bär, W. Ebeling, B. Lindner, and L. Schimansky-Geier, Eur. Phys. J. Special Topics **202**, 1 (2012).
[2] M. C. Marchetti, J. F. Joanny, S. Ramaswamy, T. B. Liverpool, J. Prost, M. Rao, and R. Aditi Simha, Rev. Mod. Phys. **85**, 1143 (2013).
[3] C. Bechinger, R. Di Leonardo, H. Löwen, C. Reichhardt, G. Volpe, and G. Volpe, Rev. Mod. Phys. **88**, 045006 (2016).
[4] S. Ramaswamy, J. Stat. Mech. 054002 (2017).
[5] É. Fodor, and M. C. Marchetti, Physica A **504**, 106 (2018).
[6] F. Schweitzer, *Brownian Agents and Active Particles: Collective Dynamics in the Natural and Social Sciences*, Springer: Complexity, Berlin, (2003).
[7] *E. Coli in Motion*, H. C. Berg, (Springer Verlag, Heidelberg, Germany) (2004).
[8] M. E. Cates, Rep. Prog. Phys. **75**, 042601 (2012).
[9] D. L. Blair, T. Neicu, and A. Kudrolli, Phys. Rev. E **67**, 031303 (2003).
[10] L. Walsh, C. G. Wagner, S. Schlossberg, C. Olson, A. Baskaran, and N. Menon, Soft Matter **13**, 8964 (2017).
[11] J. Toner, Y. Tu, and S. Ramaswamy, Ann. of Phys. **318**, 170 (2005).
[12] N. Kumar, H. Soni, S. Ramaswamy, and A. K. Sood, Nature Comm. **5**, 4688 (2014).
[13] T. Vicsek, A. Czirók, E. Ben-Jacob, I. Cohen, and O. Shochet, Phys. Rev. Lett. **75**, 1226 (1995).
[14] S. Hubbard, P. Babak, S. Th. Sigurdsson, and K. G. Magnússon, Ecological Modelling, **174**, 359 (2004).
[15] Y. Fily, and M. C. Marchetti, Phys. Rev. Lett. **108**, 235702 (2012).
[16] J. Palacci, S. Sacanna, A. P. Steinberg, D. J. Pine, and P. M. Chaikin, Science **339**, 936 (2013).
[17] A. B. Slowman, M. R. Evans, and R. A. Blythe, Phys. Rev. Lett. **116**, 218101 (2016).
[18] J. Schwarz-Linek, C. Valeriani, A. Cacciuto, M. E. Cates, D. Marenduzzo, A. N. Morozov, and W. C. K. Poon, Proc. Natl. Acad. Sci. USA **109**, 4052 (2012).

[19] G. S. Redner, M. F. Hagan, and A. Baskaran, Phys. Rev. Lett. **110**, 055701 (2013).
[20] J. Stenhammar, R. Wittkowski, D. Marenduzzo, and M. E. Cates, Phys. Rev. Lett. **114**, 018301 (2015).
[21] A. P. Solon, Y. Fily, A. Baskaran, M. E. Cates, Y. Kafri,M. Kardar, J. Tailleur, Nature Phys. **11**, 673 (2015).
[22] K. Malakar, A. Das, A. Kundu, K. Vijay Kumar, A. Dhar, `arXiv:1902.04171`.
[23] U. Basu, S. N. Majumdar, A. Rosso, G. Schehr, `arXiv:1908.10624`.
[24] A. Dhar, A. Kundu, S. N. Majumdar, S. Sabhapandit, G. Schehr, Phys. Rev. E **99**, 032132 (2019).
[25] A. P. Solon, M. E. Cates, and J. Tailleur, Eur. Phys. J. Special Topics **224**, 1231 (2015).
[26] A. Pototsky, and H. Stark, Europhys. Lett. **98**, 50004 (2012).
[27] K. Malakar, V. Jemseena, A. Kundu, K. Vijay Kumar, S. Sabhapandit, S. N. Majumdar, S. Redner, A. Dhar, JSTAT 043215 (2018).
[28] U. Basu, S. N. Majumdar, A. Rosso, G. Schehr, Phys. Rev. E **98**, 062121 (2018).
[29] P. Singh and A. Kundu, J. Stat. Mech. 083205 (2019).
[30] C. Kurzthaler, S. Leitmann, T. Franosch, Scientific Reports **6**, 36702 (2016)
[31] S. Das, G. Gompper, and R. G. Winkler, New J. Phys. **20**, 015001 (2018)
[32] L. Caprinia and U. M. B. Marconi, Soft Matter **15**, 2627 (2019).
[33] F. J. Sevilla, A. V. Arzola, and E. P. Cital, Phys. Rev. E **99**, 012145 (2019).
[34] B. ten Hagen, F. Kümmel, R. Wittkowski, D. Takagi, H. Löwen and C. Bechinger, Nature Comm. **5**, 4829 (2014)
[35] S. C. Takatori, R. De Dier, J. Vermant, and J. F. Brady, Nature Comm. **7**, 10694 (2016).
[36] A. Deblais, T. Barois, T. Guerin, P.H. Delville, R. Vaudaine, J.S. Lintuvuori, J.F. Boudet, J.C. Baret, and H. Kellay, Phys. Rev. Lett. **120**, 188002 (2018).
[37] O. Dauchot and V. Démery, Phys. Rev. Lett. **122**, 068002 (2019).
[38] W. Horsthemke and R. Lefever, *Noise-Induced Transitions: Theory and applications in Physics, Chemistry and Biology*, Springer-Verlag, Berlin, (1984)
[39] V. I. Klyatskin, Radiophys. Quantum El. **20**, 382 (1978).
[40] V. I. Klyatskin, Radiofizika **20**, 562 (1977).
[41] R. Lefever, W. Horsthemke, K. Kitahara, I. Inaba, Prog. Theor. Phys. **64**, 1233 (1980).
[42] P. Hänggi, P. Jung, Adv. Chem. Phys. **89** 239, (1995).
[43] P. Pietzonka, K. Kleinbeck, and U. Seifert, New J. Phys. **18**, 052001 (2016)
[44] T. Demaerel, C. Maes, Phys. Rev. E **97**, 032604 (2018).
[45] NIST Digital Library of Mathematical Functions, F. W. J. Olver, A. B. Olde Daalhuis, D. W. Lozier, B. I. Schneider, R. F. Boisvert, C. W. Clark, B. R. Miller, B. V. Saunders, H. S. Cohl, and M. A. McClain, eds.
[46] *Table of Integrals, Series, and Products*, I.S. Gradshteyn, I.M. Ryzhik, Academic Press (1943).